

Supporting Information

Zinc-Catalyzed Highly Isolelective Ring Opening Polymerization of *rac*-Lactide

Srinivas Abbina, and Guodong Du*

Department of Chemistry, University of North Dakota, 151 Cornell Street Stop 9024, Grand Forks, North Dakota 58202, United States

Email: gdu@chem.und.edu

Content	Page
Experimental Details	S2-4
Table S1. Ring Opening Polymerization of <i>rac</i> -Lactide with Catalyst 2a	S5
Figure S1: GPC chromatogram of PLA generated by catalyst 2a (50 °C)	S6
Figure S2: GPC chromatogram of PLA generated by catalyst 2a (75 °C)	S6
Figure S3: MALDI-TOF spectrum of PLA generated by catalyst 2a	S7
Figure S4: MALDI-TOF spectrum of PLA generated by catalyst 2a +BnOH	S7
Figure S5: Homonuclear decoupled ¹ H NMR spectra of the methine region of PLAs	S8
Figure S6: ¹³ C NMR of PLA obtained from ROP of <i>rac</i> -lactide using catalyst 2g	S9
Figure S7: ¹³ C NMR of PLA obtained from ROP of <i>rac</i> -lactide	S10
Figure S8: Plot of <i>rac</i> -LA conversion vs time	S10
Figure S9: Dependence of PLA formation on catalyst (2a) concentration.	S11
Figure S10: Plot of ln(<i>k</i> _{obs}) vs ln[Zn] for ROP of <i>rac</i> -LA by 2a at 35 °C	S11
Figure S11: Eyring plot of ln(<i>k</i> /T) vs 1/T	S12
Figure S12: Plot of <i>P</i> _m vs conversion during the ROP of <i>rac</i> -LA by 2a	S13
Figure S13: Comparison of rates of ROP of <i>rac</i> -LA vs <i>L</i> -LA	S13
Figure S14: DSC curve of PLA generated by catalyst 2a , at 50 °C	S14
Figure S15: DSC curve of PLA generated by catalyst 2b , at 50 °C	S14
Figure S16: Correlation between <i>T</i> _m and <i>P</i> _m of Isotactic PLAs	S15
References	S15

Experimental Section

General Considerations. All reactions with air- and/or moisture sensitive compounds were carried out under dry nitrogen atmosphere using a glove box or standard Schlenk line techniques. All chemicals were purchased from Aldrich unless noted otherwise. *rac*-Lactide and (*L*)-lactide ((3*S*)-*cis*-3,6-dimethyl-1,4-dioxane-2,5-dione) were recrystallized from ethyl acetate and sublimed four times prior to use. CDCl₃ and dichloromethane (DCM) were distilled over CaH₂ and degassed prior to use. Toluene and tetrahydrofuran (THF) were distilled under nitrogen from Na/benzophenone. Zinc bis(trimethylsilyl)amide¹ and the amido-oxazolate zinc complexes² were synthesized following the literature procedure.

The NMR spectra were recorded on a Bruker AVANCE-500 NMR spectrometer (¹H, ¹³C, and homonuclear decoupled ¹H NMR) and were referenced to the residual solvent. The microstructures of PLA samples were characterized by examination of the methine region in the homonuclear decoupled ¹H NMR spectra recorded at room temperature in CDCl₃ with concentrations in the range 1 to 1.5 mg/mL. Five different stereo errors for PLA, *rmr*, *mmr/rmm*, *mmr/rmm*, *mmm*, and *mrmm*, are typically observed in the region between 5.15-5.25 ppm on homonuclear decoupled ¹H NMR spectra after decoupling the methane protons of the PLA. *P_m* values of the PLAs are determined by $P_m = 1 - P_r$, where $P_r = 2[(rmr, mmr/rmm)]/[rmr, mmr/rmm + mmr/rmm, mmm, mrmm]$ according to the literature.³ The base line corrections in homonuclear decoupled NMR spectra were performed using cubic spline fitting. Matrix-assisted laser desorption/ionization time-of-flight mass spectrometry (MALDI-TOF MS) spectra were run on an Applied Biosystems/MD SCIEX 4800 MALDI TOF/TOF instrument. An accelerating voltage of 6 kV was applied and spectra were recorded in a reflector mode. The polymer samples were dissolved in THF at a concentration of 1 mg/mL. The matrix agent α -cyano-4-

hydroxycinnamic acid was used and dissolved in THF at the concentration of 40 mg/mL. Sodium acetate was used as a cationization agent at the concentration of 5 mg/mL in THF. The final matrix solution was prepared in the volume ratio of 4:4:1 of solutions of matrix, polymer, and salt respectively. A small amount of the solution was hand-spotted on a stainless steel plate and dried. This plate was loaded in instrument and spectra were recorded.

Gel permeation chromatography (GPC) analysis was performed on a Varian Prostar instrument equipped with a PLgel 5 μ m Mixed-D column and a Prostar 355 Refractive Index (RI) detector, using THF as eluent at a flow rate of 1 mL/min (20 °C). Polystyrene standards were used for calibration. Differential scanning calorimetry (DSC) measurements were obtained on a Perkin Elmer Jade differential scanning calorimeter and the instrument was calibrated using zinc and indium standards. Melting points (T_m) of the polymer samples were determined from the second heating cycles with a heating/cooling rate of 5 °C/min under nitrogen atmosphere (20 mL/min). DSC data were analyzed using Pyris V9.0.2 software. The reported T_m values are the average of three runs; all of the individual runs were from the second heating cycles of fresh PLA samples.

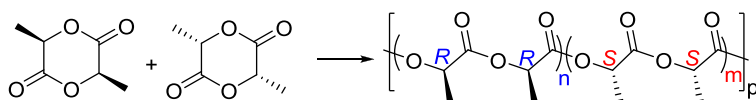
General Procedure for ROP of *rac*-Lactides: A flame dried Schlenk flask was charged with a mixture of catalyst (1 mol%) and *rac*-lactide in toluene (30-45 mL) in a Glove box. The flask was maintained at desired temperature using an oil bath (for above room temperature) controlled with a thermo couple. The stirring was continued till nearly complete conversion was observed by ^1H NMR spectroscopy. Small aliquots of the reaction mixture were collected at different time intervals and quickly quenched with DCM to characterize the polymer samples with NMR spectroscopy. At the end of the reaction, the reaction mixture was slightly concentrated in *vacuo* and quenched with THF (8-12 mL). An excess amount of MeOH (30-50 mL) was added to precipitate out the polymer. The precipitated PLA was isolated by filtration/decantation and

further dried in *vacuo* till constant weight was obtained. The same procedure was used for ROP of *cis*-lactide.

A Specific Example: Synthesis of PLA using Catalyst 2a. A flame dried Schlenk flask was loaded with a mixture of catalyst **2a** (47 mg, 0.088 mmol, 1 mol%) and *rac*-lactide (1275 mg, 8.84 mmol) in toluene (45 mL) in a glove box. The flask was heated to 50 °C and stirred for 30 min. The conversion (98 %) of the monomer into polymer was confirmed by ¹H NMR spectroscopy. The reaction mixture was first concentrated in *vacuo* and then quenched with THF (10 mL). The polymer was precipitated from addition of MeOH (35 mL). After filtration, the polymer was dried in *vacuo* until constant weight was noted, and the isolated yield of PLA was determined to be 89 %. Molecular weight of the polymer was measured by GPC and the tacticity was determined by homonuclear decoupled ¹H NMR as described earlier.

Procedure for Kinetic Experiments. In a typical run, a flame dried Schlenk flask was loaded with a solution of catalyst **2a** (46 mg, 0.086 mmol, 1 mol%) in toluene (6.0 mL) in a glove box. To this solution, a solution (67.0 mL) of *rac*-lactide (1240 mg, 8.62 mmol) in toluene was added. The flask was heated to desired temperature and small aliquots were collected at regular intervals to determine the conversion of the monomer. The conversion-time profile followed approximately first order kinetics up to 85% conversion. The apparent first order rate constants (k_{obs}) were determined by the single exponential fit of the conversion-time profile, or by the linear fit of the semilogarithm plot of lactide concentration vs. reaction time. The dependence on catalyst (**2a**) concentration was determined at 35 °C using [*rac*-LA] = 0.118 M and [**2a**] in the range of 0.49 mM – 1.77 mM. Activation parameters of the polymerization reaction were obtained from the Eyring plot with [*rac*-LA] = 0.118 M and [**2a**] = 1.18 mM in the temperature range of 23-55 °C.

Table S1. Ring Opening Polymerization of *rac*-Lactide with Catalysts 2a-2g^a



entry	cat	solvent	T (°C)	time	conv. (%) ^b	M _n (GPC) (kg/mol) ^c	M _n (calcd) (kg/mol) ^d	Đ ^c	P _m ^e	T _m (°C) ^f	k _m /k _r ^g
1	2a	toluene	23	13 h	91	49.0	13.4	1.29	0.81	189	4.3
2	2a	toluene	50	30 min	98	30.0	14.1	1.30	0.77	176	3.3
3	2a	toluene	75	15 min	93	3.6	13.4	1.14	0.76	179	3.2
4	2a	toluene	0	72 h	94	59.2	13.5	1.19	0.90	214	9.0
4-a	2a	toluene	0	72 h	94	61.4	13.5	1.21	0.89 (0.87)	215	8.1
5	2a	THF	50	30 min	84	3.2	12.1	1.03	0.71	172	2.4
6	2a	DCM	41	30 min	89	31.9	12.8	1.13	0.78	175	3.5
7 ^g	2a	toluene	50	30 min	95	40.1	27.4	1.13	0.80	208	4.0
8	2a	bulk	130	8 min	91	45.5	13.1	1.15	0.77	-	3.3
9 ^h	2a	toluene	50	10 h	93	3.9	13.4	1.10	0.61	-	1.6
10 ⁱ	2a	toluene	50	125 min	91	34.5	13.1	1.12	1.0	168	-
11	2b	toluene	50	30 min	96	18.0	13.8	1.07	0.76 (0.76)	184	3.2
12	2c	toluene	50	30 min	96	30.2	13.8	1.10	0.80	195	4.0
13	2d	toluene	50	30 min	97	28.0	14.0	1.18	0.67 (0.70)	170	2.2
14	2e	toluene	50	30 min	80	29.4	11.5	1.05	0.72	194	2.6
15	2f	toluene	50	30 min	95	21.2	13.7	1.37	0.78	196	3.5
16	2g	toluene	50	30 min	93	37.4	13.4	1.23	0.86 (0.82)	204	6.1
17	2g	toluene	23	44 h	96	52.2	13.8	1.32	0.91 (0.89)	212	10.1

^aReactions were carried out using 1 mol% of catalyst at 50 °C in toluene, unless noted otherwise. ^bMonomer conversion determined by ¹H NMR.

^cExperimental molecular weight determined by GPC vs polystyrene standards in THF. The values are corrected by a factor of 0.58. ^dCalculated molecular weight based on conversion and catalyst loading. ^eProbability of *meso* (P_m) enchainment, determined by the integration of methine region of the homonuclear decoupled ¹H NMR. The P_m values in parenthesis were determined on the basis of ¹³C NMR.⁵ ^fDetermined by DSC. The values are averages of three duplicates. ^g1:200 ratio of catalyst:monomer is used. ^hBnOH (1 mol%) was employed as cocatalyst ⁱL-lactide was used.

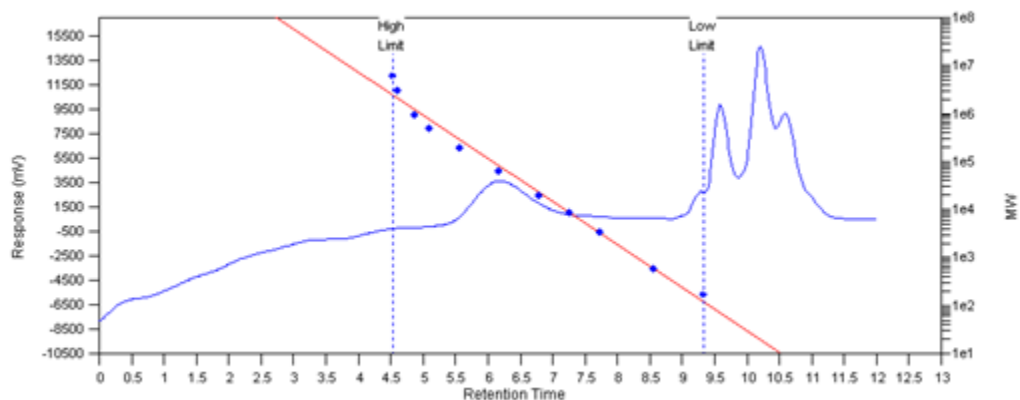


Figure S1: GPC chromatogram of PLA generated by catalyst **2a** (50 °C). The additional peaks at the longer retention times are from the solvent.

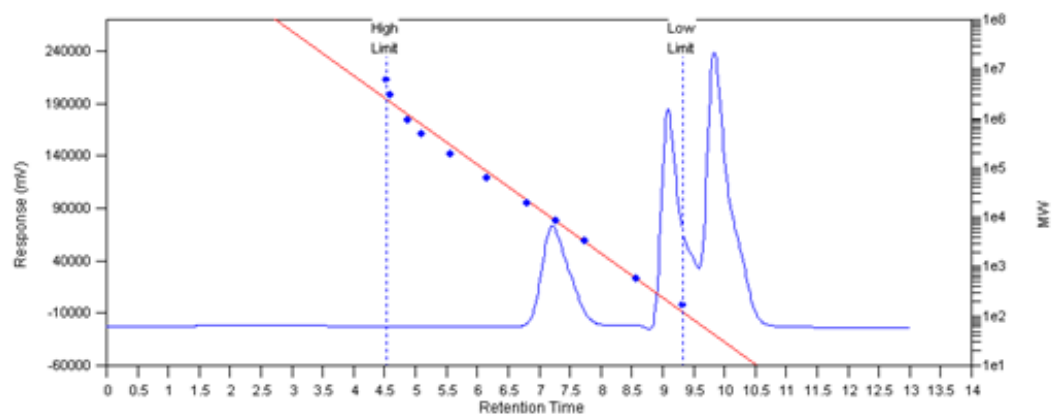


Figure S2: GPC chromatogram of PLA generated by catalyst **2a** (75 °C). The additional peaks at the longer retention times are from the solvent or *rac*-LA monomer.

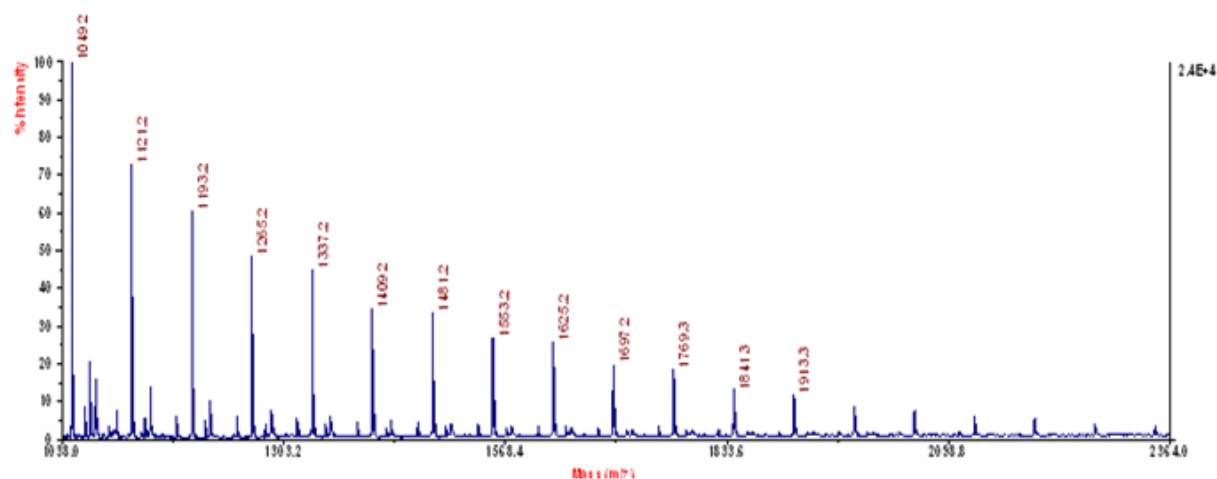


Figure S3: MALDI-TOF spectrum of PLA generated by catalyst **2a** (entry 1, table 1), showing predominantly PLA capped with the $\text{N}(\text{SiMe}_3)_2$ end group ($M_n = 72.02 n + 160.10$ ($-\text{N}(\text{SiMe}_3)_2$) + 22.99 (Na^+)).

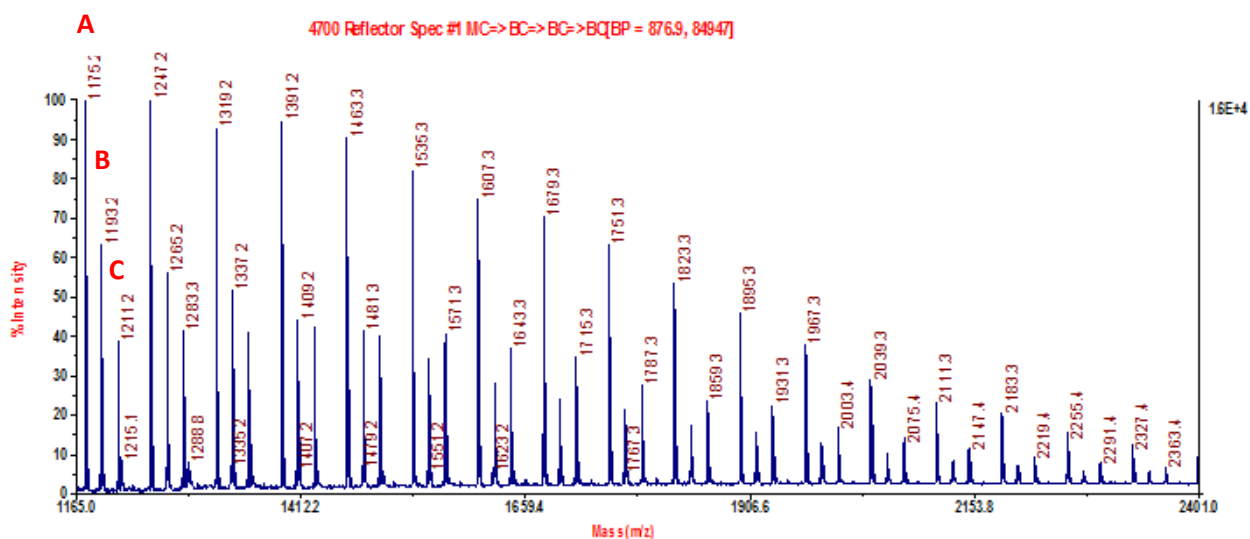
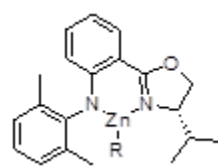
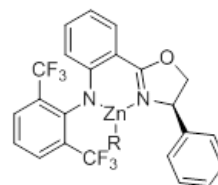
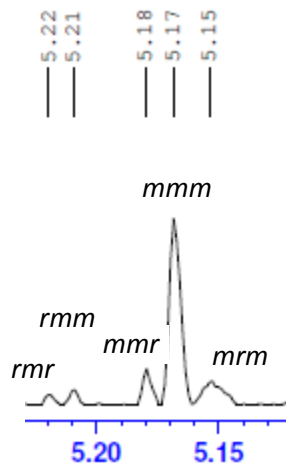


Figure S4: MALDI-TOF spectrum of PLA generated by catalyst **2a**+BnOH at $50\text{ }^\circ\text{C}$ (entry 9, Table 1), showing PLAs capped with $\text{N}(\text{SiMe}_3)_2$ (**B**; $M_n = 72.02 n + 160.10$ ($-\text{N}(\text{SiMe}_3)_2$) + 22.99 (Na^+)) and benzoxyl (PhCH_2O) (**C**; $M_n = 72.02 n + 107.13$ (PhCH_2O) + 22.99 (Na^+)) end groups, as well as cyclic PLAs (**A**; $M_n = 72.02 n + 22.99$ (Na^+)).



2a, $P_m = 0.90$ (0°C)



2g, $P_m = 0.91$ (23°C)

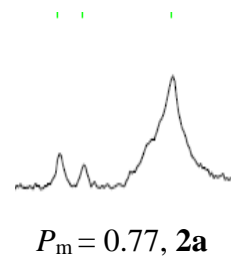
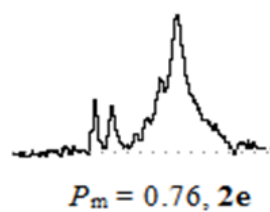
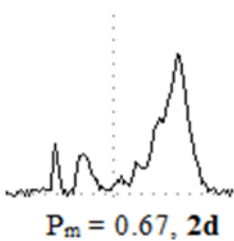
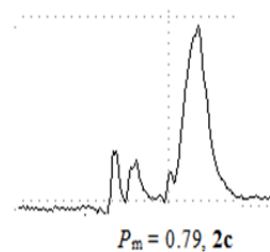
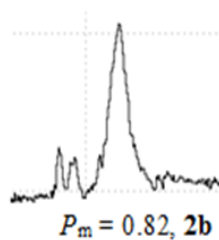
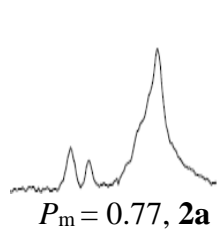
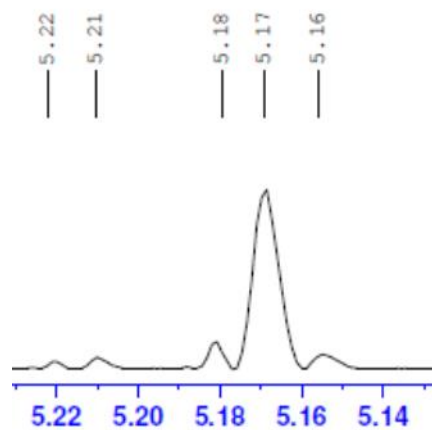


Figure S5: Homonuclear decoupled ^1H NMR spectra of the methine region of PLA generated from *rac*-LA using Zn catalysts **2a-2g**. The reactions were carried out in toluene at 50°C unless noted otherwise.

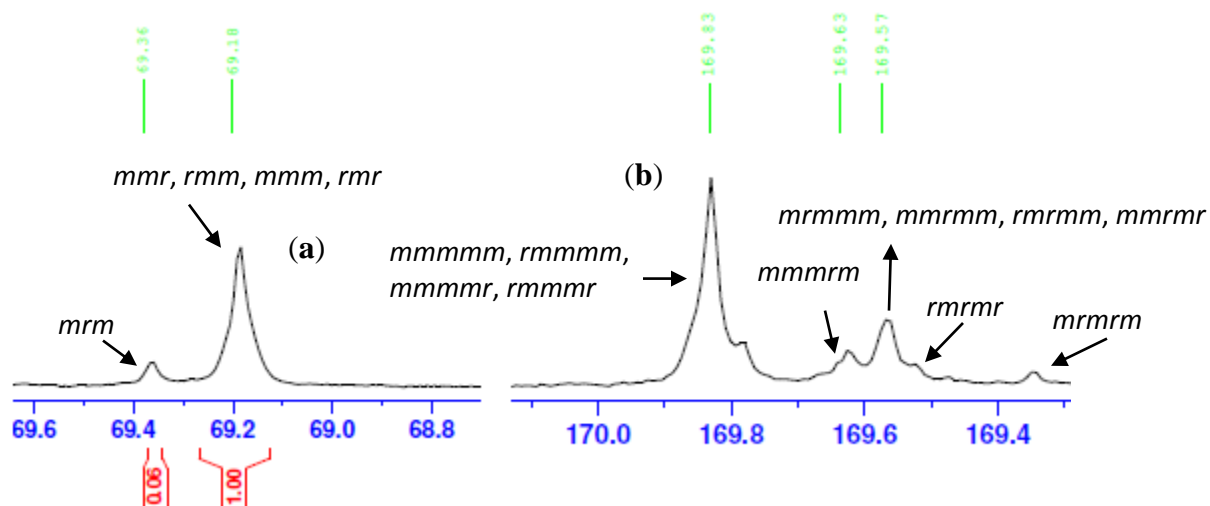


Figure S6: ^{13}C NMR spectrum of PLA obtained from ROP of *rac*-lactide using catalyst **2g** at ambient temperature (23 °C) showing the tetrads in the methine region (a) and the hexads in the carbonyl region (b). The P_m value determined from ^{13}C NMR for this sample is 0.89, comparable to the result from the determination by homonuclear decoupled ^1H NMR ($P_m = 0.91$). The probability of formation of a meso linkage (P_m) of PLA can be derived from the methine region of ^{13}C NMR spectrum as follows (Bernoullian statistics):⁵

$$(1-P_m)/2 = [mrm]/([mrm]+[mmm] +[mmr]+[rmm]+[rmr])$$

$[mmm]$	$P_m(P_m+1)/2$
$[mmr]$	$P_m(1- P_m)/2$
$[rmm]$	$P_m (1-P_m)/2$
$[rmr]$	$(1-P_m)^2/2$
$[mrm]$	$(1-P_m)/2$

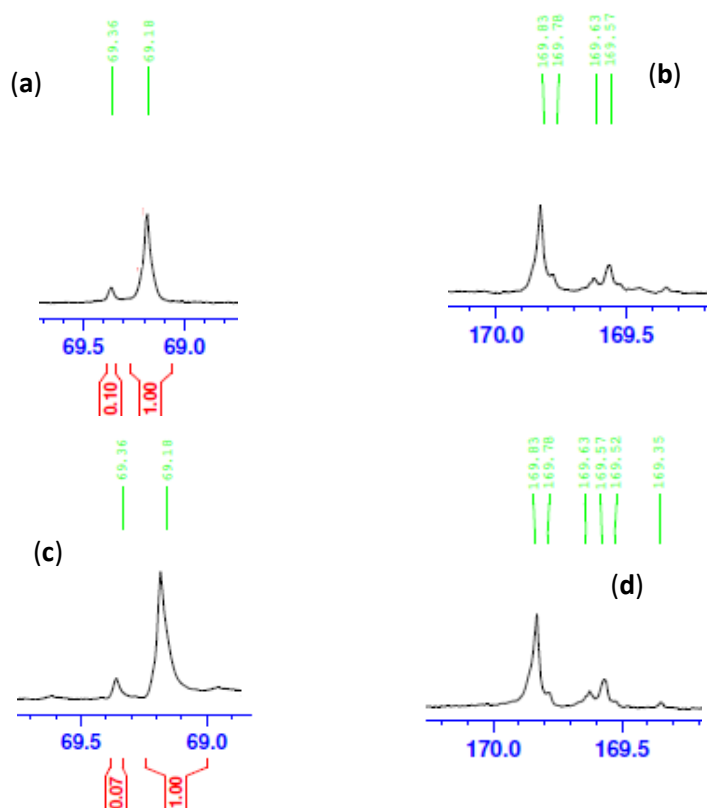


Figure S7: ^{13}C NMR spectra showing the tetrads in the methine region (a) and the hexads in the carbonyl region (b) of PLA obtained from ROP of *rac*-lactide using catalyst **2g** at 50 °C; and the tetrads in the methine region (c) and the hexads in the carbonyl region (d) of PLA obtained from ROP of *rac*-lactide using catalyst **2a** at 0 °C.

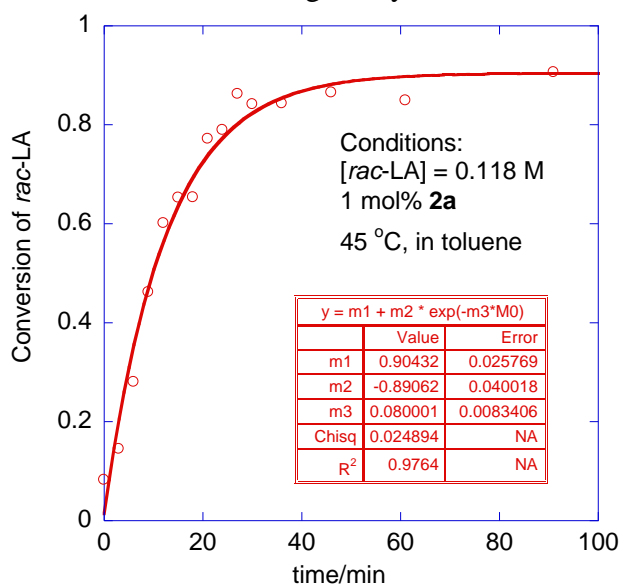


Figure S8: Plot of *rac*-LA conversion vs time. Exponential fitting gives a first order rate constant of $k_{obs} = 0.080 \pm 0.008 \text{ min}^{-1}$.

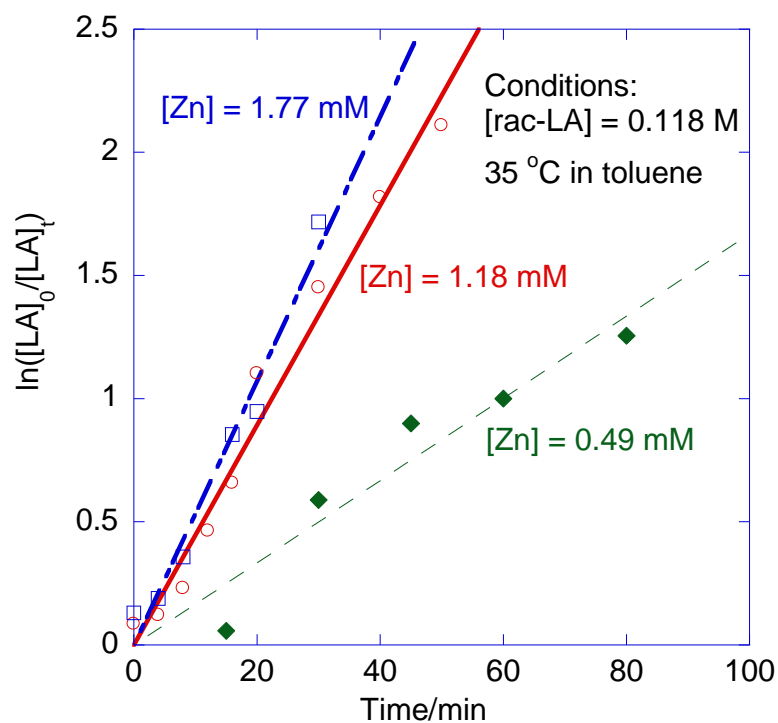


Figure S9: Dependence of PLA formation on catalyst (**2a**) concentration.

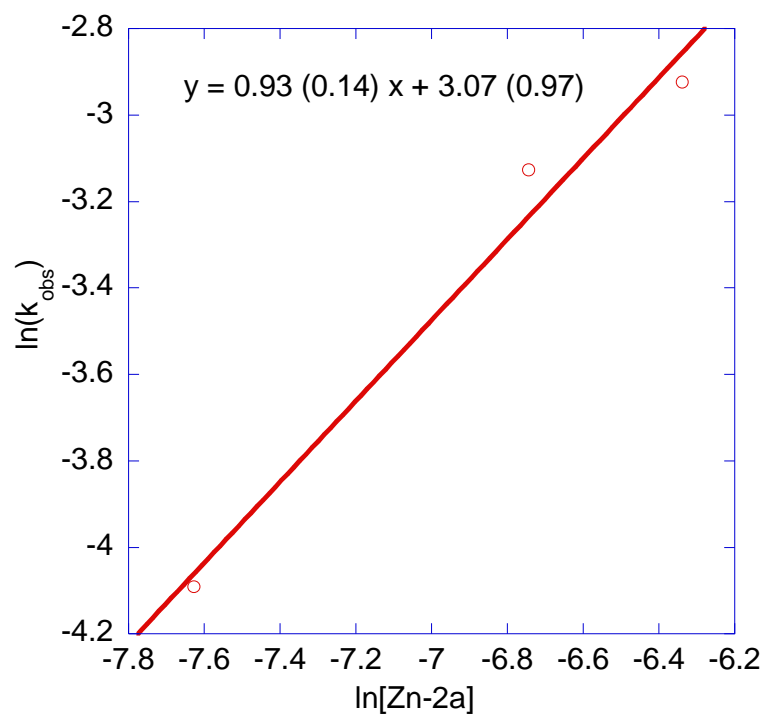


Figure S10: Plot of $\ln(k_{obs})$ vs $\ln[Zn]$ for ROP of *rac*-LA by **2a** at 35°C in toluene, which gives the reaction order on $[Zn]$ of $0.93 (\pm 0.14)$. The unit for k_{obs} is min^{-1} .

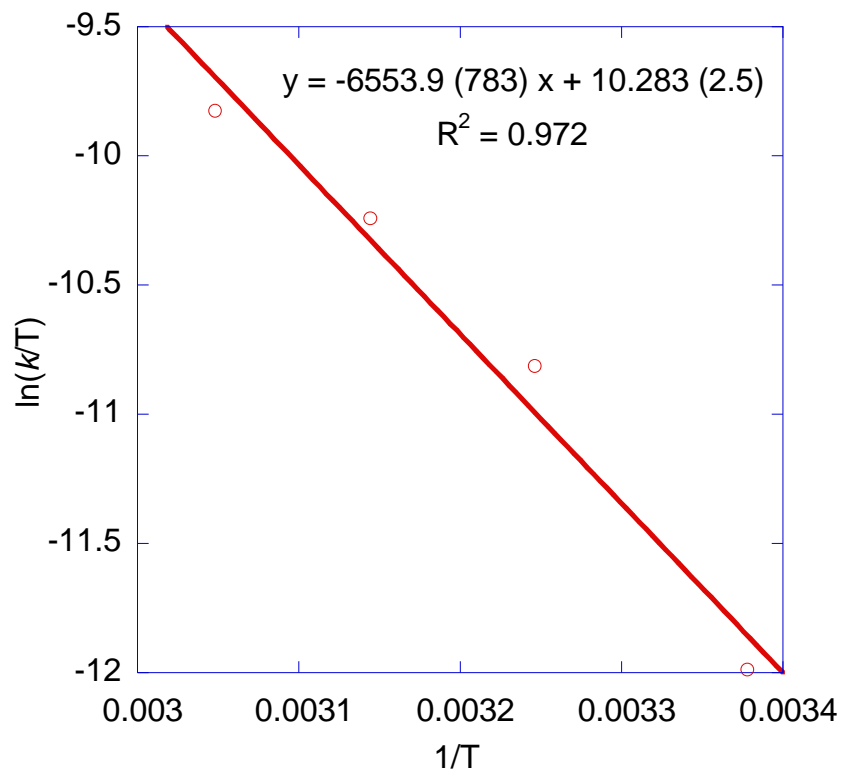


Figure S11: Eyring plot of $\ln(k/T)$ vs $1/T$ gives a straight line (shown in Figure 1) with $y = -6553.9 (783) x + 10.283 (2.5)$, $R^2 = 0.972$ from which $\Delta H^\ddagger = 54 (\pm 7) \text{ kJ mol}^{-1}$ and $\Delta S^\ddagger = -112 (\pm 21) \text{ J mol}^{-1} \text{ K}^{-1}$ were derived. The rate data used are listed in the following table.

T/K	$k_{\text{obs}} / \text{min}^{-1}$	$k_{\text{obs}} / \text{s}^{-1}$	$k / \text{mol}^{-1} \text{s}^{-1}$	$1/T$	$\ln(k/T)$
296	0.013	0.000217	0.001836	0.003378	-11.9904
308	0.0438	0.00073	0.006186	0.003247	-10.8155
318	0.080001	0.001333	0.01130	0.003145	-10.245
328	0.1252	0.002087	0.01768	0.003049	-9.82813

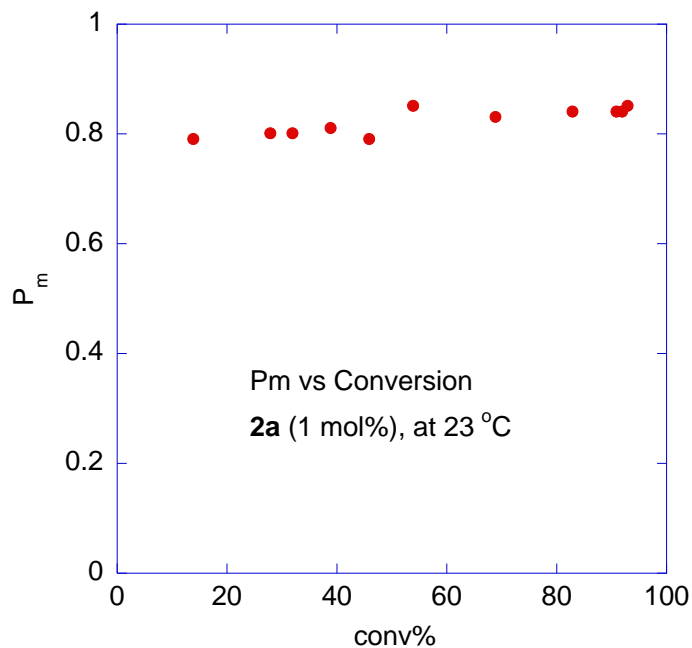


Figure S12: Plot of P_m vs conversion during the ROP of *rac*-LA by **2a** at 23 °C.

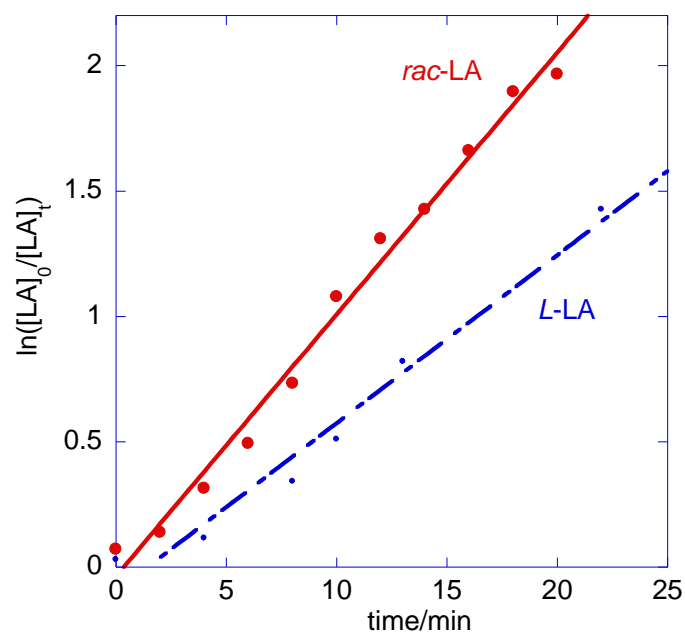


Figure S13: Comparison of rates of ROP of *rac*-LA vs *L*-LA. Conditions: $[LA] = 0.11$ M, 1 mol% of **2a**, in toluene, 55 °C. $k_{rac-LA}/k_{L-LA} = 1.6$.

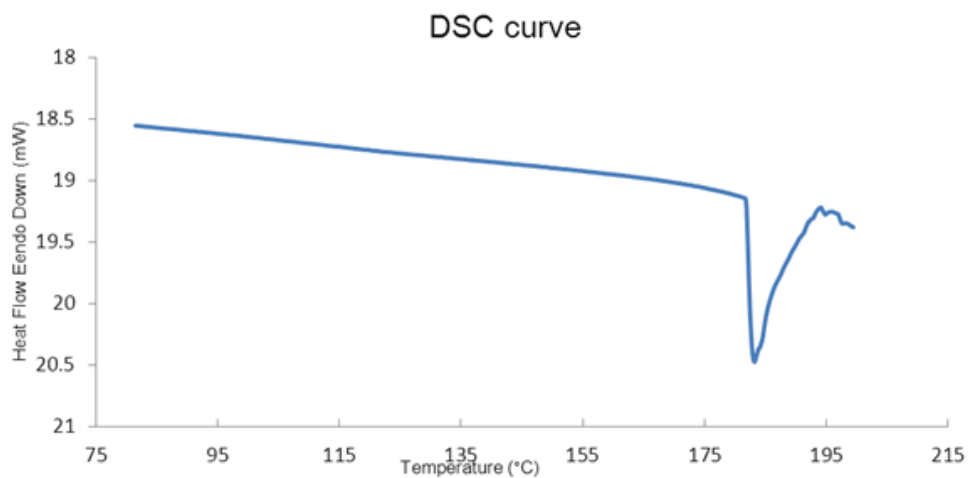


Figure S14: DSC curve of PLA generated by catalyst **2a** at 50 °C ($T_m = 183$ °C)

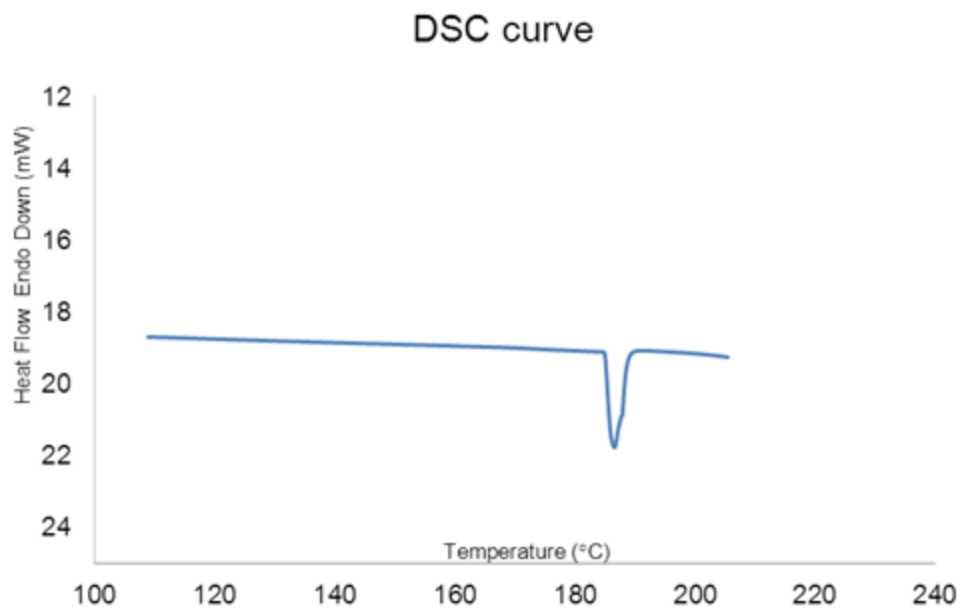


Figure S15: DSC curve of PLA generated by catalyst **2b** at 50 °C ($T_m = 186$ °C)

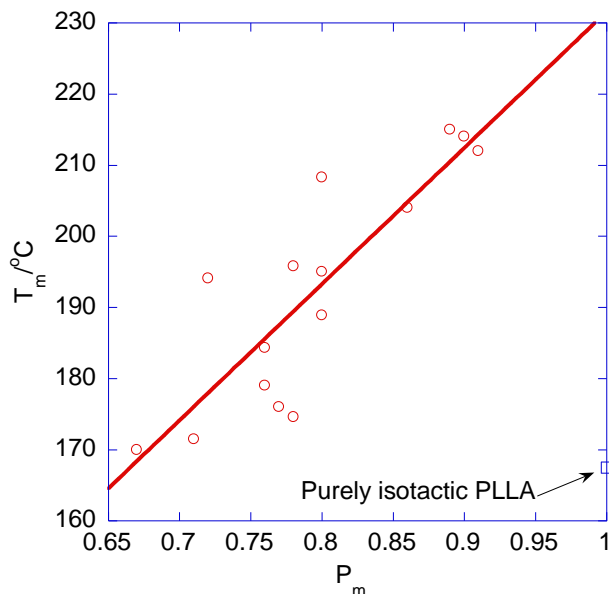


Figure S16: Correlation between T_m and P_m of Isotactic PLAs obtained in this study ($R^2 = 0.72$).

References

- ¹ Darensbourg, D. J.; Holtcamp, M. W.; Struck, G. E.; Zimmer, M. S.; Niezgoda, S. A.; Rainey, P.; Robertson, J. B.; Draper, J. D.; Reibenspies, J. H. *J. Am. Chem. Soc.* **1999**, *121*, 107–116.
- ² Abbina, S.; Du, G. *Organometallics* **2012**, *31*, 7394–7403.
- ³ Drouin, F.; Oguadinma, P. O.; Whitehorne, T. J. J.; Prud'homme, R. E.; Schaper, F. *Organometallics* **2010**, *29*, 2139–2147.
- ⁴ Du, H.; Pang, X.; Yu, H.; Zhuang, X.; Chen, X.; Cui, D.; Wang, X.; Jing, X. *Macromolecules* **2007**, *40*, 1904–1913.
- ⁵ (a) Makiguchi, K.; Yamanaka, T.; Kakuchi, T.; Terada, M.; Satoh, T. *Chem. Commun.* **2014**, *50*, 2883–2885. (b) Nomura, N.; Hasegawa, J.; Ishii, R. *Macromolecules* **2009**, *42*, 4907–4909. (c) Chamberlain, B. M.; Cheng, M.; Moore, D. R.; Ovitt, T. M.; Lobkovsky, E. B.; Coates, G. W. *J. Am. Chem. Soc.* **2001**, *123*, 3229–3238.